

The ALFOSC camera

Properties of the W11-3 CCD

Anton Norup Sørensen & Preben Nørregaard
Copenhagen University Observatory

October 1996

1 Introduction

For the commissioning of the Andalucia Faint Object Spectrograph and Camera (ALFOSC) at the Nordic Optical Telescope (NOT) in October 1996, the instrument is temporarily equipped with a camera containing a CCD of less than desirable quality. In this document, the properties of this CCD mounted in the ALFOSC camera are described.

The CCD is a Ford-Loral three side buttable with 2048^2 imaging pixels, serial number W11-3. Packaging for back-side illumination, thinning and coating was performed by the Steward Observatory CCD Laboratory. The CCD requires UV-flooding for any significant blue sensitivity.

The CCD was in 1995 installed in the camera for the DFOSC at La Silla. The dewar suffered from a sudden puncture a short time after installation, exposing the cold CCD to ambient air. Condensation of water-ice damaged the coating, and the chip was taken back to Copenhagen University Observatory (CUO). Since then the CCD has been used for test purposes, including baking at 130°C , a further accidental oil contamination, washing in aggressive chemicals, student exercises and much more. While it has got several scars from these experiences, the CCD has proven to be very sturdy and performing fairly well. It has been selected for the ALFOSC commissioning primarily to gain experience on the performance of ALFOSC, but it is also hoped to be able to produce data of an acceptable quality until a replacement chip arrives.

2 Operating options

The CCD has two functional output amplifiers, 'A' and 'B'. These can be selected individually or used simultaneously. Default is 'A' only. The cross-talk between the amplifiers during simultaneous read-out is around 1:30000.

The parallel phases can be operated in "normal" or "mpp" mode. No differences in performance between these modes has been observed in the CUO lab, but measurements at the telescope indicated otherwise. Please investigate!

Operating temperature is normally -100°C , and testing has only been performed at this temperature.

Two ADU conversion factors can be selected, "high" or "low". "high" gain is default and offers the best signal to noise ratio at the expense of a slightly reduced dynamic range.

The area to be read out may be specified by any rectangular section, and on-chip pixel binning may be specified independently in the x and y directions.

3 Cosmetics

The spatial structure of the flat fields is rather strong, as described in more detail in the section on UV-flooding. The CCD has an unusually small number of pixels affected by charge traps.

The only major defect is a hot column area, affecting X=1993-5. Several minor traps exists, but a map of these has not been made.

4 Read-out noise

Noise measured in bias frames amounts to:

	Amplifier A	Amplifier B
High gain:	6.5 e ⁻	6.6 e ⁻
Low gain:	7.2 e ⁻	8.0 e ⁻

5 Gain, linearity and full-well

From analysis of photon noise statistics, the following conversion factors were found:

	Amplifier A	Amplifier B
High gain:	1.02 e ⁻ /ADU	1.07 e ⁻ /ADU
Low gain:	2.8 e ⁻ /ADU	3.0 e ⁻ /ADU

Gain measured from noise has a dependency on the exposure level of up to 5% on some CUO cameras. For the W11-3, the relation found is plotted in figure 1. These measurements were made using another controller than the current, though. Direct measurements of ADUs versus exposure time has shown the camera to be linear to within 0.3%. An example of a crude version of this measurement is given in figure 2. The apparent gain variation is thus not a real effect, but indicate that the gain values tabulated here may be in error by a few percent.

The cause for the deviation in noise statistics is not known, but for a candidate, see the section on the analog to digital converter.

An independent measurement using a ⁵⁵Fe X-ray source gave 1.045 e⁻/ADU for amplifier A in high gain mode.

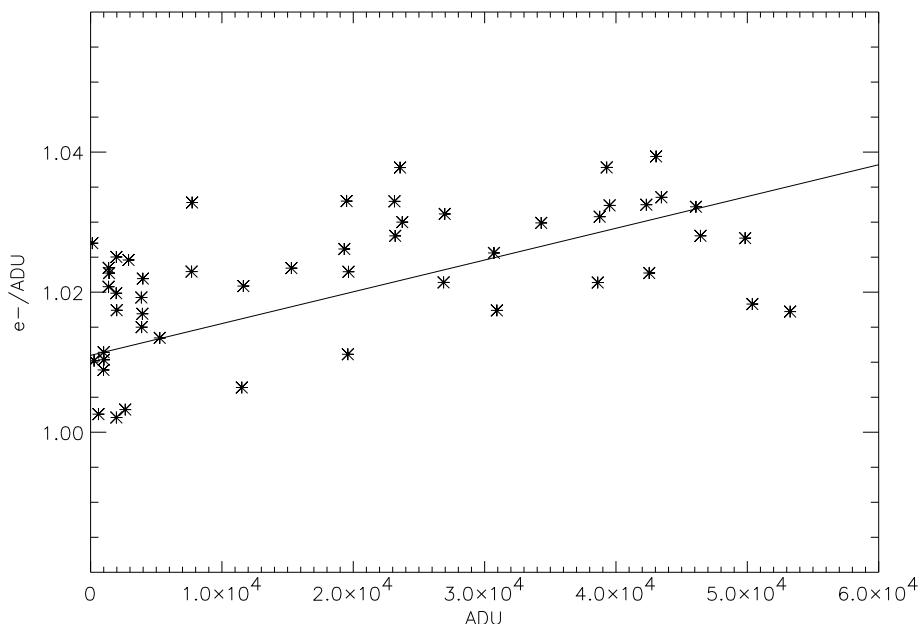


Figure 1: Gain versus exposure level measured from noise statistics for amplifier A in high-gain, but with another controller than the currently used. About two percent of deviation from linearity is indicated, but this is shown to be false by direct measurements.

Full well: No saturation effects are seen at 110.000 e⁻, corresponding to 40.000 ADU in low-gain mode and above the ADU range in high gain mode. This value was found both in “normal” and “mpp” mode. Above 120.000 e⁻, the signal is strongly influenced by hardware saturation.

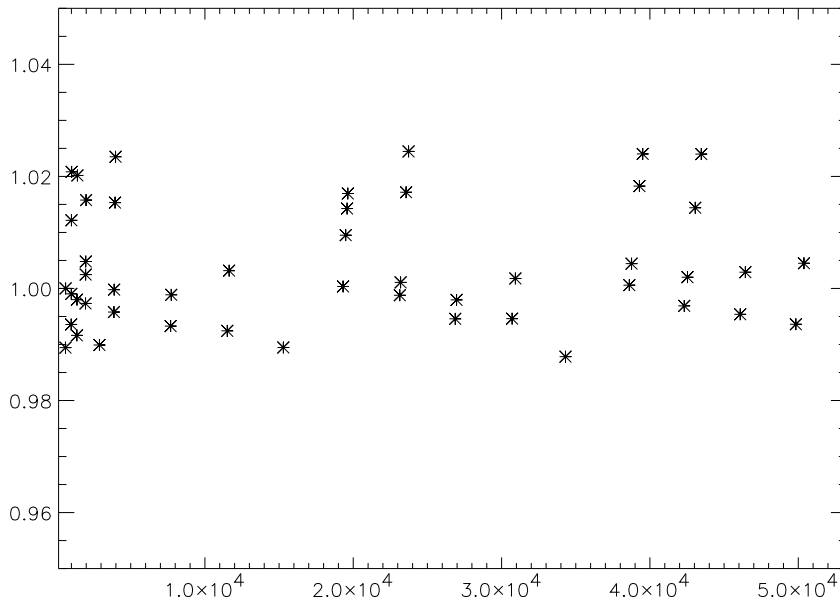


Figure 2: A plot of ADU per second versus total exposure time, corrected for shutter delay. The main uncertainty is from drift in the light source intensity. Tracking of the intensity decreases the spread to 0.3% with no indication of linearity deviation.

6 Charge transfer efficiency

The fraction of electrons that are successfully moved from one pixel to another during read-out is described by the charge transfer efficiency (CTE).

The CTE has been measured using a ^{55}Fe X-ray source, whose emissions generate a specific number of photo-electrons on the CCD for each detection. The read-out counts as a function of position on the CCD can then be converted to a CTE value.

The values found are:

Serial CTE: 0.999997

Parallel CTE: 0.999997

Transporting the charge from the most remote corner of the CCD to the output amplifier will then lead to a 1.3% loss of charge

Note that CTE strictly speaking is a function of exposure level, so the value given here may not be applicable to all cases. Near zero level and full well, CTE can be expected to be poorer.

7 MTF

No measurements of the spatial resolution of this chip has been made, but it is expected to suffer from MTF degradation due to diffusion of the photo-electrons. The diffusion will be small at near-infrared wavelengths and increase to maximum level at wavelengths shorter than 500nm. For similar devices, a spread of around two pixels FWHM has been found.

8 UV-flooding and quantum-efficiency

The QE of W11-3 after UV-flooding is NOT stable in time and structure!

Only if high QE at short wavelengths is essential, and high precision photometry is not needed, UV flooding can be applied.

Procedure for UV-flooding:

Let the camera heat up to room temperature by setting the CCD reference temperature to $+20^{\circ}\text{C}$ before the remaining liquid Nitrogen is used. As strong outgassing occurs, the camera should be pumped during the heating and must be pumped for at least an hour when warm. The camera is then filled with dry air to about ambient pressure. In order to ensure no other air enters, a T-tube must be connected to the dewar valve with the the other ends going to the dry air bottle and a vacuum pump. If the pump is not equipped with a valve, one must be inserted. The tube between the the cryostat and bottle is then evacuated, the valve to the cryostat opened, removing outgassing components from the warm camera. The valve to the pump is closed, and dry air can now slowly be let in while monitoring the camera pressure closely. Fill the camera to slightly less than ambient pressure, then close the cryostat valve. The UV-flooding lamp is placed approx. 3 centimeters in front of the camera window, and the CCD is illuminated for half an hour, including lamp warm-up time. After flooding, the camera must be pumped for about an hour before filling with LN_2 .

Stability of the UV-flooded sensitivity: The change in time of the average QE in the central region is shown in figure 3. A rapid decay immediately after flooding is seen. In order to reach a more stable level, the camera was heated to room temperature without simultaneous evacuation, and cooled again after one day. The QE is still decaying after this treatment, but at a moderate rate of about 2% per week. This procedure of flooding followed by a warm period is recommended for any observations requiring high blue sensitivity.

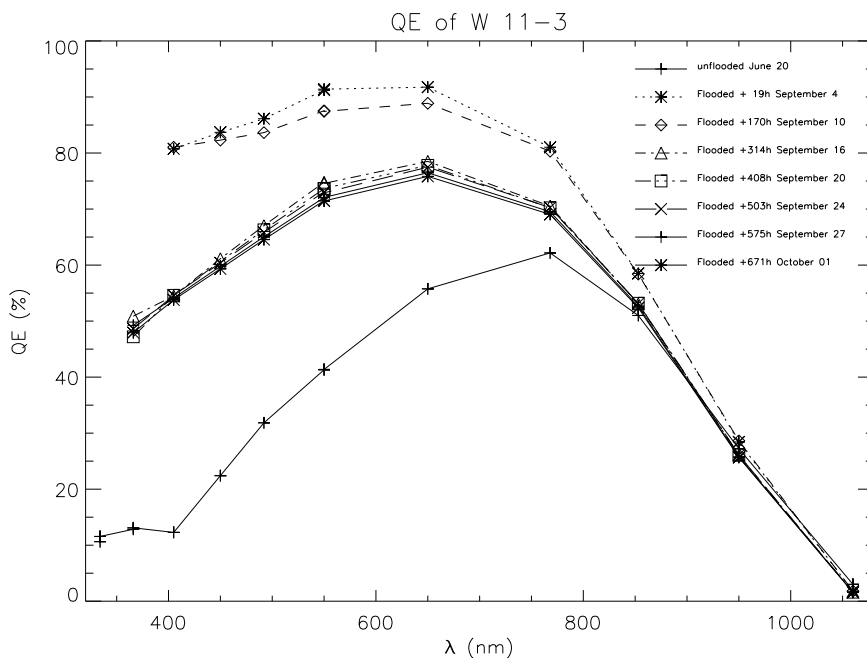


Figure 3: Quantum efficiency decay with time, as observed for W11-3. A rapid decrease is seen immediately after flooding. Between September 10 and 14, the camera was left warm for one day. Afterwards, the decay is slower, but still noticeable over a few days.

Flat field images at 1060nm, 550nm and 366nm illumination were obtained regularly after flooding. Local QE structure changes even more rapidly than the global, resulting in severe flat fielding problems shortly after flooding. Here, images from 20 and 27 days after flooding followed by a one day warm period are compared. In figures 4, 5 and 6, the spatial structure can be seen to be rather strong, mainly due to the local differences in flooding decay speed. The ratio of the images indicate a modest change in structure in time in the central area.

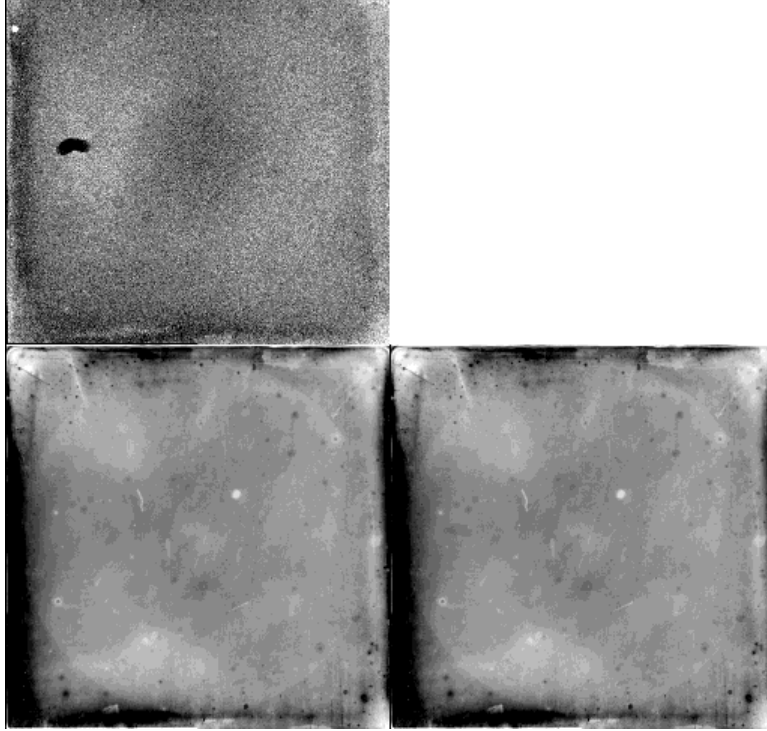


Figure 4: Flat field properties at 1060nm. *Lower left:* September 24. The greyscale area includes sensitivity within 20% of the median level. *Lower right:* October 1, 7 days later. *Upper left:* Ratio of the two flat fields. The greyscale area includes sensitivity within 1% of the median ratio. The maximum spatial difference is 0.3% when excluding the dust speck.

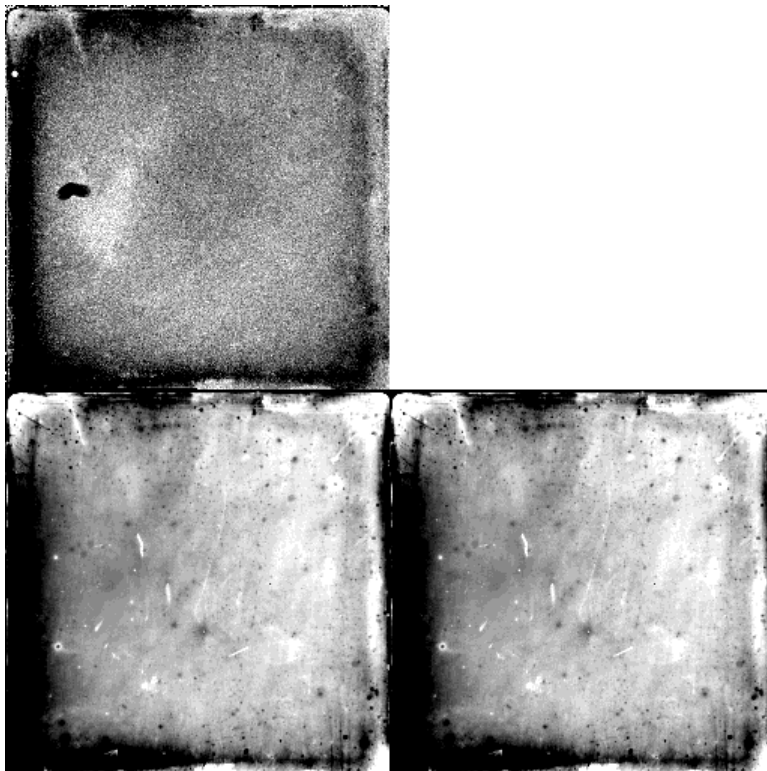


Figure 5: Flat field properties at 550nm. *Lower left:* September 24. The greyscale area includes sensitivity within 20% of the median level. *Lower right:* October 1, 7 days later. *Upper left:* Ratio of the two flat fields. The greyscale area includes sensitivity within 1% of the median ratio. The spatial difference is 0.5% at the bright patch and reaches a maximum of 3% at the left border.

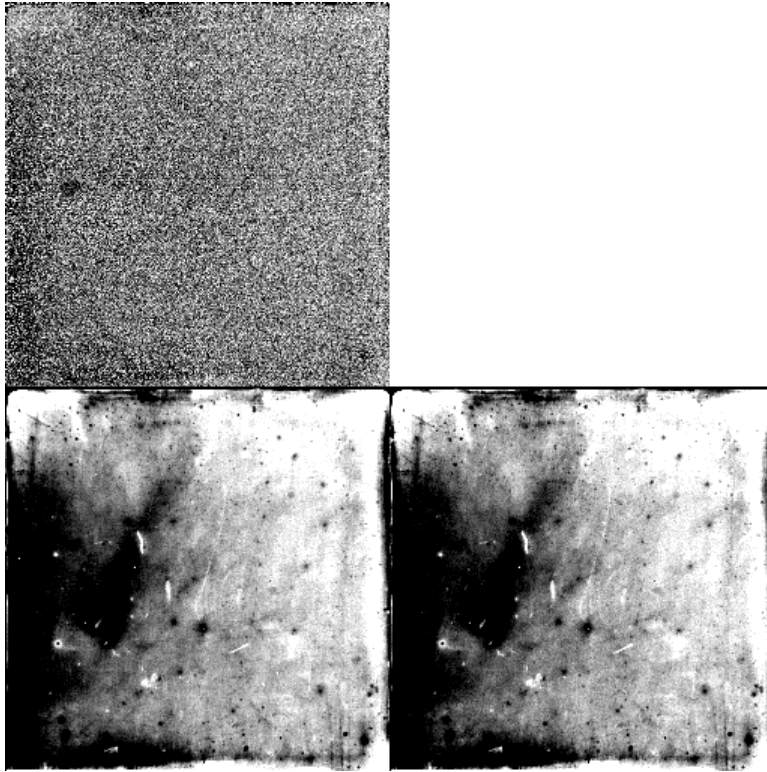


Figure 6: Flat field properties at 366nm. *Lower left:* September 24. The greyscale area includes sensitivity within 20% of the median level. *Lower right:* October 1, 7 days later. *Upper left:* Ratio of the two flat fields. The greyscale area includes sensitivity within 5% of the median ratio. Graininess is due to a poor signal to noise ratio of the exposures. The spatial difference reaches a maximum of 3% at the left border.

9 Bias and overscan

The bias level exhibits a dependency on the temperature of the electronics. As the temperature converges towards different levels during read-out and idle/integrating mode, the bias level and structure becomes a function of the exposure time of the current and previous exposures. This complex behaviour, of which an example is given in figure 7, makes overscan correction of the bias subtraction essential for low-level exposures. The CCD has a hardware overscan region of two columns at each end of the serial register. As this area is somewhat too small and is suspected to be affected by the illumination of the imaging area, an artificial overscan region was added during commissioning. Now, read-out is continued to a total of 2050 columns when operating in full-frame mode. The reliability of the artificial overscan has yet to be confirmed. The overscan region is always the last section to be read out, and thus appears in different positions depending on the output amplifier selection.

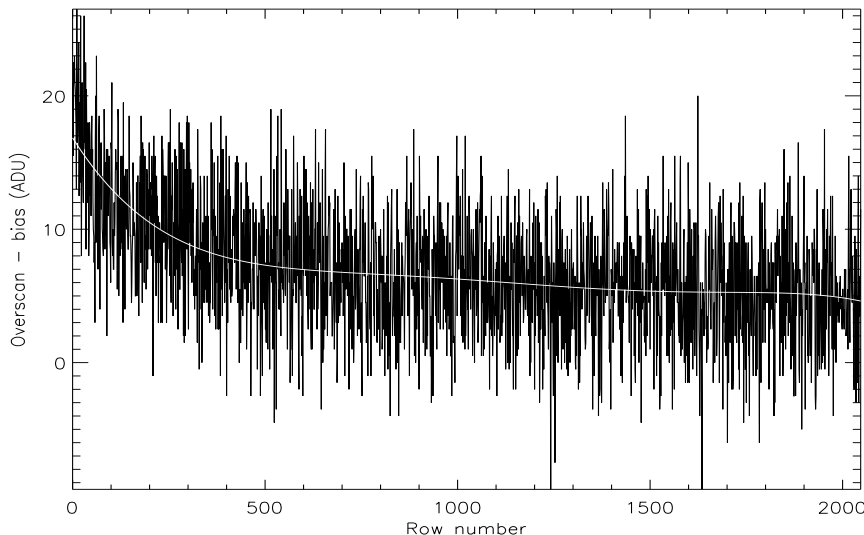


Figure 7: Overscan plot of a 20 minute dark frame, using only two columns of the “real” overscan region. As the read-out circuit has been idle for a long time, temperature changes drastically when read-out is initiated, causing a change in bias level. The overscan structure is effectively a function of the previous idle/read-out history of the camera.

10 Dark current

A dark exposure is shown in figure 8. The image is cleaned for cosmic hits and bias and overscan have been subtracted. Except for a group of hot columns at $x=1993-5$, no dark current is detected. From this, an upper limit to the dark current of $1e^-/h$ at the operating temperature of -100° C is estimated, provided overscan subtraction behaves nicely. No difference between dark exposure level and structure has been observed in “normal” and “mpp” mode.

11 Analog to Digital Converter

Imperfections in the digitization of the CCD output voltage are causing some ADU values to appear more frequently than others, as can be seen in figure 9. The additional noise may be detectable on exposures with very little signal, where the noise normally would be read-out-noise limited. With a few hundred counts or more, the photon noise will dominate the noise from the ADC.

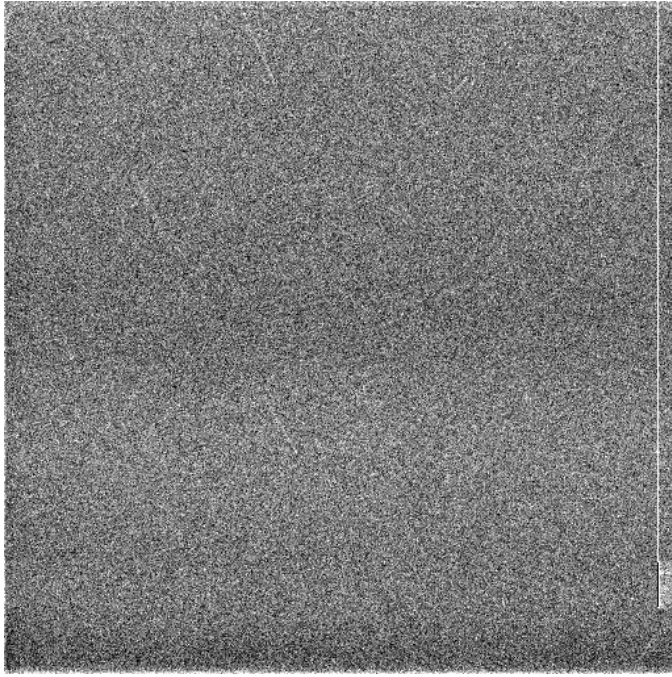


Figure 8: A median image of three 20 minute dark exposures, filtering out most cosmic hits. Bias image and overscan structure are subtracted. Except for a group of hot columns, no dark current is detected.

12 Pixel size

Illuminating the CCD with collimated light through a grid of pinholes with known separation, the following dimensions were found for a CCD from the same batch as W11-3:

Pixel size in serial direction: $15.03 \pm 0.02 \mu m$

Pixel size in parallel direction: $14.99 \pm 0.01 \mu m$

This is consistent with the design specifications of $15 \mu m$ square pixels.

13 Cryostat

The holding time of the cryostat is relatively short, between 12 and 18 hours, due to the orientation of the dewar. The filler opening is pointing slightly downwards, so the inner tube should always be inserted, which will allow filling the dewar to a bit more than half of the capacity.

The pressure in the dewar is measured by a Pirani gauge and the output is interpreted and displayed by a auxiliary electronics box. The gauge and display are calibrated for each other - changing one of the components can result in very misleading output. In spite of the calibration, the display of pressures below 10^{-3} mBar are somewhat deviating. The Pirani output has been compared to the outputs from Penning sensors of two different brands, which are more reliable in this pressure range. The relation between Penning and Pirani pressure is shown in figure 10.

The dewar is equipped with a activated charcoal sieve, which will help to keep the vacuum when cold. The operating pressure should be below 10^{-3} mBar. If the pressure goes above this, the camera must be pumped for a while. If the temperature in the dewar goes above -50° C, the camera must be allowed to heat to room temperature and pumped for an hour before cooling again. UV-flooding will decay rapidly during the warm period, so re-flooding should be considered.

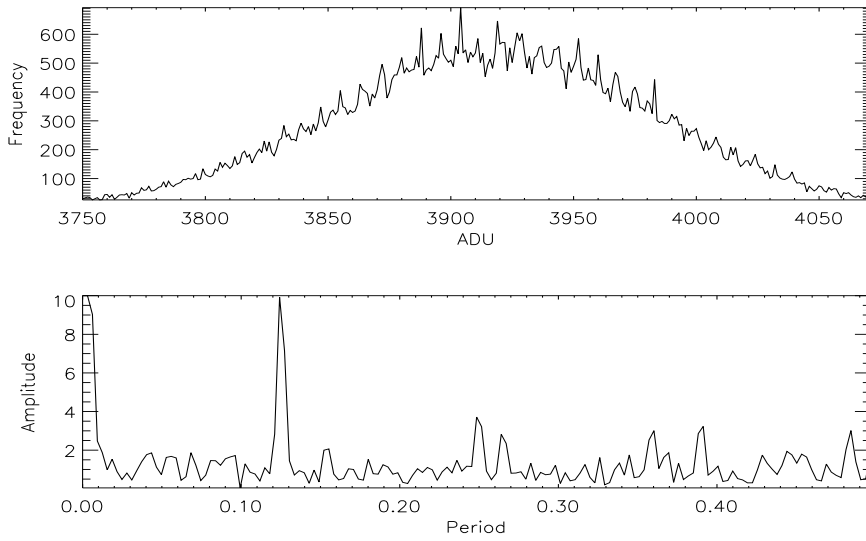


Figure 9: *Upper*: Histogram of a flat-field exposure. *Lower*: Frequency spectrum of the histogram. The ADU levels are seen to be modulated, in particular every eighth value seems to appear with increased frequency. This is caused by errors in the digitization process.

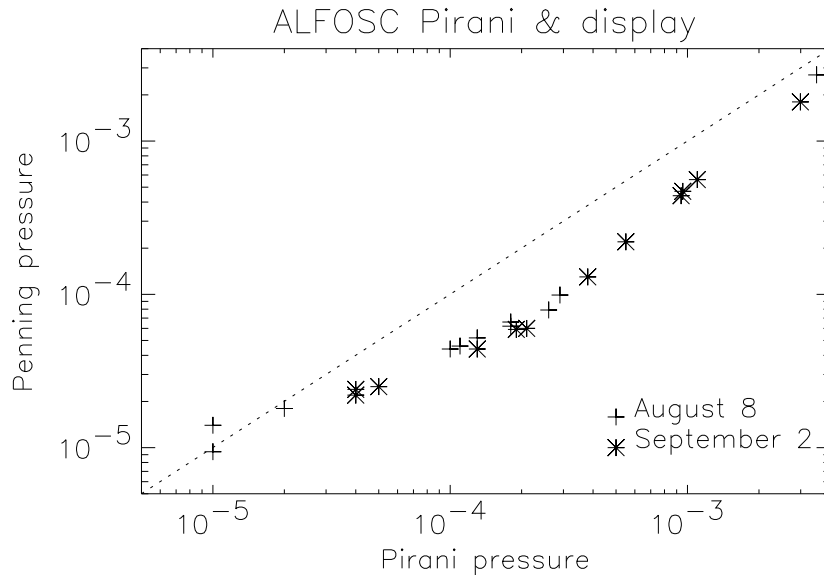


Figure 10: ALFOSC Pirani sensor pressure versus Penning sensor pressure. The calibration performed on August 8 seems still to be valid nearly a month later.